# Development and performance of graphene oxide reinforced LDPE nanocomposite polymers for 3D printing

http://dx.doi.org/10.1590/0370-44672023770059

**Bryan M. M. Silva**[1,2]
https://orcid.org/0000-0002-7815-569X
**Caroline C. Tegon**[1,3]
https://orcid.org/0000-0001-5155-2698
**Marcelo M. Soares**[1,4]
https://orcid.org/0000-0001-7143-2255
**Rodolfo Luiz Prazeres Gonçalves**[1,5]
https://orcid.org/0000-0001-5183-4636
**Andressa A. Oliveira**[1,6]
https://orcid.org/0000-0002-0362-9918
**Antonio Augusto Couto**[1,7]
https://orcid.org/0000-0003-1503-1582
**Marcos Massi**[1,8]
https://orcid.org/0000-0002-7117-8039

[1]Universidade Presbiteriana Mackenzie, Escola de Engenharia, São Paulo – São Paulo - Brasil.

E-mails: [2]b.mm.silva@hotmail.com,
[3]caroltegon@gmail.com, [4]marcelomelo61@gmail.com,
[5]rodolfo.luiz99@gmail.com, [6]andressa_120@hotmail.com,
[7]antonioaugusto.couto@mackenzie.br,
[8]marcos.massi@mackenzie.br

## Abstract

This study evaluated the mechanical properties and the chemical and thermal characteristics of low-density polyethylene (LDPE) nanocomposites reinforced with graphene oxide for manufacturing via 3D printing. LDPE nanocomposites with different graphene oxide (GO) loadings (0.5% and 1.5%) were processed by a single-screw extruder. To characterize the pre-injected material, Fourier transform infrared spectroscopy (FTIR) and thermal characterization with thermogravimetry (TGA) were used. The injected material was also characterized with mechanical impact and traction tests. The results showed that incorporating GO into the polymeric matrix added hydroxyl groups to the matrix structure, with a 39.13% increase in Young's modulus for LDPE-1.5%wtGO samples. Mechanical tests of 3D printed samples showed that, with an increase in the amount of GO in the polymer matrix, the composite loses ductility, enabling its use in 3D printing technologies and thus encouraging new studies on printed materials for various applications.

**Keywords:** low-density polyethylene (LDPE), graphene oxide (GO), 3D printing.

## 1. Introduction

The growing demand for customized and simple processing parts with reduced costs has driven many studies in the manufacture of composite materials, especially those related to additive 3D printing technologies. These technologies have enabled the manufacture of complex and customized parts for various applications. However, the search for suitable materials for these technologies continues to be a significant challenge (Qassemyar *et al*., 2017).

Polyethylene has great industrial importance as one of the most widely used polymers. Low-density polyethylene (LDPE) stands out as an economical and easily processable material (AL-Ammari *et al*., 2019; Callister, 1991; Gahlot & Kulshrestha, 2019; Lee *et al*., 2019; Trivedi *et al*., 2022; Yusof *et al*., 2023) with exceptional resistance to acids, bases, solvents, and recyclability (Olesik, Godzierz, and Kozioł, 2019; Trivedi *et al*., 2022). However, LDPE has some limitations related to low wear resistance, susceptibility to stress cracking, relatively low strength, and stiffness. When subjected to 3D printing processing, it demonstrates poor adhesion to printing beds and high shrinkage, limiting its use in the pure state by this type of processing (Boczkowska & Krzesinski, 2016; Sleziona, 1998).

To overcome these limitations, some studies have developed LDPE-based polymer matrices reinforced with different materials (Olesik, Godzierz and Kozioł, 2019). In this context, graphene oxide (GO) is an interesting and promising reinforcement for making composites (Nagi *et al.*, 2020; Hou *et al.*, 2017). GO is a material with unique characteristics and can improve the mechanical properties of polymer-based composites (Cao, Y, *et al.*, 2001; Rafiee, M, *et al.*, 2009) in addition to presenting hydroxyl and carboxyl functional groups, which can improve the interfacial bonding with the polymer matrix. Furthermore, at the nanoscale, material properties are influenced by surface chemistry and reinforcement size, making it suitable to produce nanocomposites (Tibbetts *et al.*, 2007). Trivedi (2022) comments that polymer nanocomposites have the potential to replace conventional materials due to their processability through various techniques, including 3D printing. These materials feature greater tensile strengths, improved thermal distortion temperatures, and better noise dampening than traditional materials, thus making them candidates for future industrial applications.

Already consolidated polymer processing techniques, such as injection, extrusion, compression or transfer, and blow molding, prove to be effective for manufacturing polymeric nanocomposites. However, additive manufacturing technologies through 3D printing have emerged as a new and exponent technique to produce parts with complex geometries directly from the desired material. For this growing technology, investigations in this area, with different types of materials and reinforcements, are still under development for challenges related to the process parameters and performance of these materials for the targeted applications.

This study aims to develop, evaluate, and characterize low-density polyethylene (LDPE) polymer nanocomposites, reinforced with graphene oxide and printed by 3D additive manufacturing. The specific objective was to investigate the influence of the amount of reinforcement in the structure of the preprinted material and the mechanical properties of the final printed composite.

## 2. Experimental procedures

The materials used in this study were LDPE EF2222, supplied by Braskem, which has a low gel content, ensuring good processability, with reduced film thickness and high uniformity, and graphene oxide, which was synthesized in the laboratory using the modified Hummers method, as characterized in detail by Tegon (2021) in a parallel study. Three samples of LDPE were used – pure LDPE, LDPE-0.5%wtGO, and LDPE-1.5%wtGO. The development of this research consisted of the preparation, processing, and characterization of pure LDPE and additive LDPE samples.

To manufacture the nanocomposites, two extrusion processes were carried out. A single-screw extruder with three temperature zones was used, which was fed through a hopper with gravity action.

First Extrusion: GO was mixed with pure LDPE to obtain pellets. It was worked at 33% of the maximum torque of the equipment and screw rotation of 20 rpm. The temperatures in each of the extruder zones were Zone 1 (feed): 170 °C; Zone 2 (compression): 180 °C; and Zone 3 (dosing): 190 °C.

Second Extrusion: To conform the filament diameter to 1.75 mm for 3D printing, 31% of the maximum torque of the equipment and a screw rotation of 12 rpm were used. The temperatures in each extrusion zone were the same as the first extrusion.

Injection of the specimens: For the tensile and impact tests, the injection of the specimens was carried out using the Haake mini jet pro from Thermo Scientific, following the heating cylinder temperature process parameters: 200 °C; mold temperature: 60 °C; injection pressure: 140 bar; back pressure: 80 bar (pure LDPE), 70 bar (additive LDPE), with injection pressure time of 15 seconds and back pressure time of 7 seconds.

Printing parameters for 3D Printing: An S3 3D Printer – Sethi3D – 1.75 mm was used, with a layer height of 0.2 mm, filling density of 100%, printing speed of 45 mm/s, extruder temperature of 240 °C, and bed temperature of 20 °C. Super 77 (3M) was used for fixing the table.

Mechanical analysis of the injected samples was done by tensile tests under the following conditions in accordance with D638-14. A type 4 specimen was used with a test speed of 5 (0.2) ± 25% mm/min. Impact results were obtained in accordance with ASTM D256-10. A total of five specimens were used in each condition in both tests.

Infrared spectroscopy (FTIR) was used to observe specific groups of mixture components and their interactions, which were analyzed with a nominal resolution of 4 $cm^{-1}$ and scanned 32 times with a transmission limit of 4000–600 $cm^{-1}$.

The TGA tests of the samples were carried out in alumina crucibles with an oxygen atmosphere (100 ml/min). The samples were inserted into the crucibles and taken to the oven, with support connected to the precision balance. The temperature was regulated to vary over time in seconds, while the balance provided data on the mass of a sample as a function of time. For the experiment, an isotherm was used up to 30 °C, then 10 °C/min until the final temperature.

## 3. Results and discussion

### 3.1 Pallet analysis

Figure 1 shows the FTIR spectrogram of pure LDPE and samples after GO addition. In the spectroscopic profile, asymmetric and symmetric axial deformation was observed at 2,970 and 2,870 $cm^{-1}$, respectively, of C-H. Between 1450 and 1370 $cm^{-1}$, a characteristic band of angular deformation of the C-H groups ($CH_2$ and $CH_3$) and asymmetric angular deformation of $CH_2$ at 770 $cm^{-1}$ was also visible, which is in agreement with literature (Redighieri, 2006). After the addition of GO, bands in the regions from 3,400 to 3,100 $cm^{-1}$ attributed to the -OH (hydroxyl) group became visible. The band with a wavenumber close to 1100 $cm^{-1}$ is always found for C-O molecules and is related to the carbon-oxygen stretching vibration mode, according to other authors (Lorenzetti *et al.* 2005).

The addition, GO significantly increased the hydroxyl and C-O groups, giving the material hydrophilicity, an important parameter for the adhesion of the printed composite to the printing base, in 3D printers. It is vitally important that the first layer of the print is well adhered to the print base to avoid defects on the face of the material in contact with the base. Hydrophilic surfaces facilitate this adhesion, helping to prevent the printed composite from detaching and moving during the process. Printed surface quality and hydrophilicity can affect the surface quality of printed parts. Hydrophilic surfaces can lead to a uniform distribution of the printing material, improving the quality of the part, in addition to providing increased cell adhesion for possible medical and pharmaceutical applications (Lorenzetti *et al*. 2005; Yuan *et al*., 2018; Zhou *et al*., 2019).

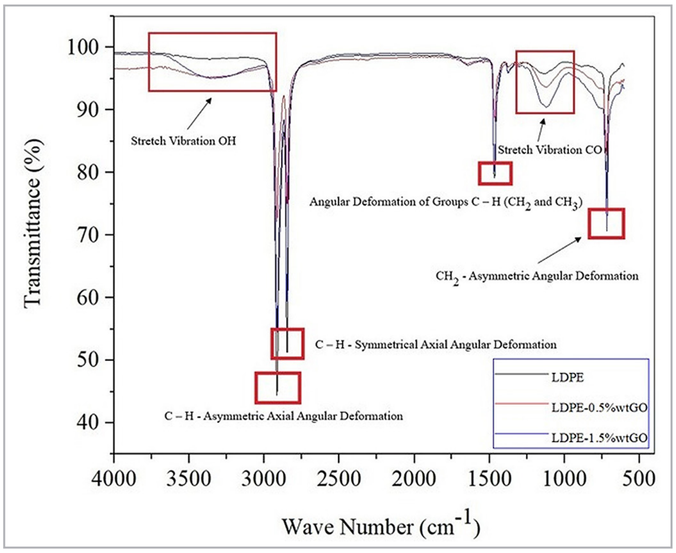

Figure 1 - FTIR graph for pure LDPE, LDPE-0.5%wtGO, LDPE-1.5%wtGO samples. FTIR spectra were obtained with a resolution of 4 cm $^{-1}$ in the 4000 to 600 cm $^{-1}$ region, where the main acquisition bands that characterize the compound are highlighted by their respective frequencies.

Figure 2 shows the graphs generated from the tensile test on pure LDPE, LDPE-0.5%wtGO, and LDPE-1.5%wtGO samples.

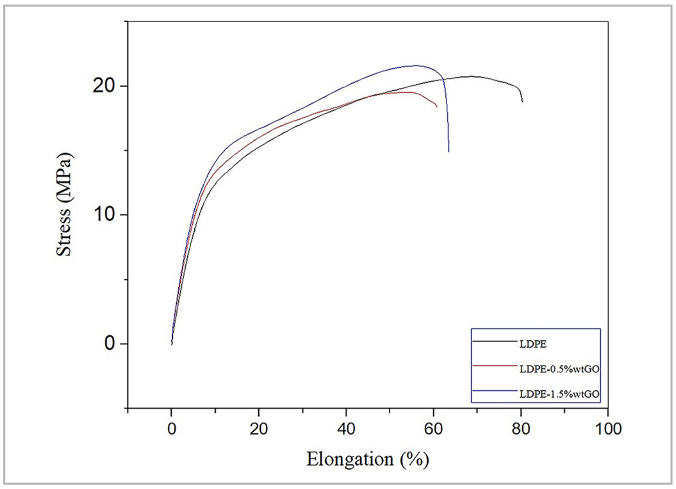

Figure 2 - Tensile tests graph for pure LDPE sample, LDPE/GO - 0.5%, LDPE/GO - 1.5%, under the conditions of standard D638 - 14 with a test speed of 5 (0.2) ± 25% mm/min.

Table 1 - Tensile test results of pure LDPE and additive LDPE.

| Series | Modulus of Elasticity (MPa) | Ultimate Tensile Strength (MPa) | Maximum Elongation (%) | Tensile Strength (MPa) | Elongation Rupture (%) |
|---|---|---|---|---|---|
| **PURE LDPE** | 276 ± 28 | 20.5 ± 2.1 | 73 ± 3 | 18.7 ± 2.1 | 80 ± 3 |
| **LDPE/0.5%wtGO** | 296 ± 46 | 19.7 ± 2.1 | 55 ± 7 | 18.3 ± 1.8 | 62 ± 5 |
| **LDPE/1.5%wtGO** | 384 ± 63 | 21.6 ± 0.6 | 58 ± 5 | 14 ± 3 | 64 ± 7 |

The results in Table 1 show the increase in Young's modulus of the composite with increasing GO loading in the LDPE matrix due to the high stiffness of GO (290 – 430 GPa) (Liu *et al*., 2012), compared to the LDPE base. Due to the standard deviation observed between the Pure LDPE and LDPE/0.5%wtGO samples, there was no increase in Young's modulus, although there is a tendency for an increase due to the increase in reinforcement load, as observed between

Pure LDPE and LDPE/1.5% wtGO. The LDPE/1.5%wtGO samples showed an average increase of 39.13% in their Young's modulus compared to pure LDPE, even with such a high standard deviation. The minimum Young's modulus values for the 1.5% LDPE samples are still higher than the maximum values obtained for pure LDPE, representing in this scenario an increase of 6.1%, representing an effective increase in this mechanical property. The performance of a composite is directly related to the quality of the interfacial interaction between reinforcement and matrix, associated with the aspect ratio of the filler, in addition to the functional groups available on the GO surface, as well as the proportion and dispersion of the reinforcement in the matrix. For small amounts of reinforcement or low dispersion, the elasticity parameter is not sensitive and only begins to improve with a more homogeneous dispersion and an increase in the amount of filler in the matrix (Fu *et al.*, 2008).

A decrease in the ultimate strength of the samples in LDPE-0.5%wtGO was observed in relation to pure LDPE. A weak interfacial interaction and low dispersion provide low load transfer between the matrix and reinforcement. In this case, the reinforcement becomes a stress concentrator, favoring the presence of places susceptible to rupture, leading the material to rupture with lower loads (Fu *et al.*, 2008). The LDPE-1.5%wtGO samples showed an ultimate strength of 21.6 MPa, which represents a 5.3% increase in ultimate strength. The toughness of the materials did not significantly change (Table 2). However, the decrease observed in additive materials may be related to their loss of ductility due to added fillers (Croucillo *et al.*, 2018).

Table 2 – Results of impact test on pure LDPE and additive LDPE.

| Series | Energy/Thickness (J/m) | Energy/area (J/m²) | Impact Speed (m/s) |
|---|---|---|---|
| **PURE LDPE** | 298 | 37.2 | 3.45 |
| **LDPE/0.5%wtGO** | 275 | 34.2 | 3.45 |
| **LDPE/1.5%wtGO** | 289 | 36.9 | 3.45 |

In the TGA analysis illustrated in Figure 3, the LDPE-1.5%wtGO composite presented a curve close to pure LDPE but slightly higher, with the beginning of thermal degradation of pure LDPE around 220 °C and 250 °C for LDPE-1.5%wtGO. Pandey *et al.* (2016) verified the same phenomenon using graphene as reinforcement in HDPE. They observed that the TGA curves showed the same degradation profile, with a positive displacement of the curves, when increasing the load of carbonaceous material in the direction of the increase in degradation temperature during the test. These authors concluded that when the graphene in the matrix increases, the composite acquires greater thermal stabilization, as also observed by Bu *et al.* (2016). Quiles-Díaz *et al.* (2017) reported the same phenomenon and attributed the delay in the decomposition process to the barrier effect of nanoparticles, which prevents the transport of gas-phase products of polymer decomposition. In contrast to the pure LDPE and LDPE-1.5%wtGO, the LDPE-0.5%wtGO composite showed greater thermal stability, starting its degradation at around 310 °C with an abrupt drop in mass around 415 °C. The mechanism favored thermal stability with sudden mass loss compared to pure LDPE, and the mechanism of LDPE-1.5%wtGO is not yet clear, obtaining a mass loss only slightly above that of pure LDPE; however, this mechanism will be studied in future work.

The importance of knowing the mass loss in relation to the temperature of this nanocomposite is related to the extrusion of this material in the 3D printer. After several printing attempts, this nanocomposite obtained better extrusion and adhesion on the base of the 3D printer with an extruder temperature of 240 °C and bed temperature of 20 °C. Thus, for extrusion and adhesion in the 3D printer, this nanocomposite with LDPE matrix and GO filler has a mass loss in relation to temperatures above 240 °C.

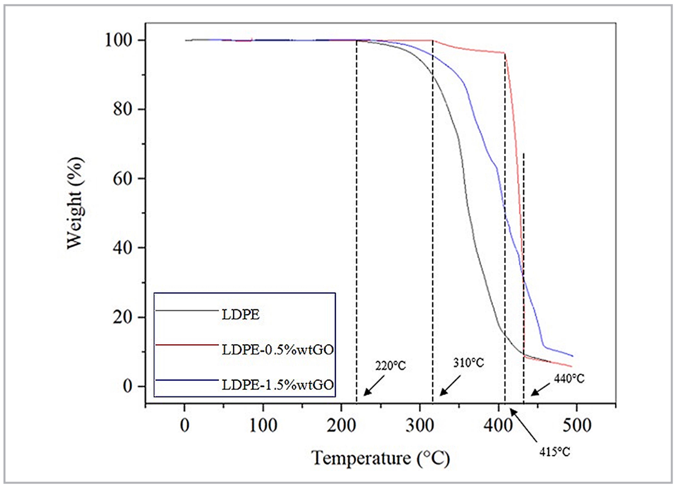

Figure 3 – TGA graphs of pure LDPE, LDPE-0.5%wtGO, LDPE-1.5%wtGO samples operated with an oxygen atmosphere (100 ml/min) and an isotherm up to 30°C, then 10°C/min until the final temperature.

### 3.2 3D printing

After mechanical tests, the pure LDPE and added LDPE filaments were inserted into the 3D printer. Pure LDPE could not be printed, possibly due to its high ductility, while the added LDPE achieved good printing performance, as seen in Figure 4. The samples with GO demonstrated satisfactory printability, where the parameters and geometries used for testing were simpler and with printing configurations and filaments similar to those of materials already commonly used, such as PLA (poly lactic acid). This calls for further investigation of the state of the art on the interaction of GO and other carbonaceous materials in 3D printable polymers for automotive, aeronautical, and medical applications.

Figure 4 – Printed samples of LDPE-0.5%wtGO (left), LDPE-1.5%wtGO (right) - with extruder temperature of 240 °C and Print Bed of 20 °C - Layer Height: 0.2 mm - Filling density: 100% - Speed: 45 mm/s.

## 4. Conclusions

This research developed GO-reinforced LDPE composites for 3D printing applications. FTIR revealed that the addition of graphene oxide significantly increased hydroxyl and CO groups. This provided the material with the necessary hydrophilicity for adhesion to the printing table and quality printed surface. Additional studies should explore applications of this material in various areas including medical and pharmaceutical applications, given the mechanical results observed. The tensile test found a considerable difference in relation to pure LDPE and LDPE-1.5%wtGO, increasing Young's modulus from 276 to 384 MPa (39.13%), consequently obtaining a reduced ductility due to the increased load from GO. This result can be important and significant for the 3D printing of parts with fine details, complex geometries, rigidity, and dimensional stability, due to the decrease in the ductility of the composite, associated with the increase in strength through the addition of reinforcement in the polymer matrix, which tends to maintain the material with better workability for 3D printing techniques.

A positive shift was observed in the TGA curves, with increasing GO load, toward increasing degradation temperature during the test, making the composite thermally more stable. It can be applied at higher temperatures in a 3D printer extruder, depending on the GO load.

## Acknowledgments

The authors would like to thank the financial support from the Brazilian Research Foundations CNPq and CAPES. They also thank the following institutions for the use of their characterization equipment: Universidade Presbiteriana Mackenzie - UPM and MackPesquisa.

## References

AL-AMMARI, R. H.; GANASH, A. A.; SALAM, M. A. Electrochemical molecularly imprinted polymer based on zinc oxide/graphene/poly(o-phenylenediamine) for 4-chlorophenoldetection. ***Synthetic Metals,*** 254, p. 141-152, 2019.

BOCZKOWSKA, A.; KRZESINSKI, G. ***Kompozyty i techniki ich wytwarzania.*** OWPW: Warszawa, Poland, 2016.

BU, J.; HUANG, X.; LI, S.; JIANG, P. Significantly enhancing the thermal oxidative stability while remaining the excellent electrical insulating property of low-density polyethylene by addition of antioxidant functionalized graphene oxide. ***Carbon***, 106, p. 218-227, 2016.

CALLISTER, W. D. Materials science and engineering: an introduction. 2. ed. ***Materials & Design,*** v. 12, n. 1, p. 59, 1991.

CAO, Y.; ZHANG, J.; FENG, J.; WU, P. Compatibilization of immiscible polymer blends using graphene oxide sheets. ***ACS Nano***, v. 5, n. 7, p. 5920-5927, 2011.

CROUCILLO, A. P. dos R. *et al.* Avaliação das características mecânicas do Pla, impressa em 3D, para aplicação em próteses em animais de pequeno e médio porte. ***Tecnologia em Metalurgia Materiais e Mineração,*** v. 15, n. 3, p. 221-225, 2018.

FU, S.-Y.; FENG, X.-Q.; LAUKE, B.; MAI, Y.-W. Effects of particle size, particle/matrix interface adhesion and particle loading on mechanical properties of particulate–polymer composites. ***Composites Part B: Engineering,*** v. 39, n. 6, p. 933-961, 2008.

GAHLOT, S.; KULSHRESTHA, V. Graphene based polymer electrolyte membranes for electro-chemical energy applications. ***International Journal of Hydrogen Energy,*** 2019.

HOU, Y.; DUAN, L.; GUI, Z.; HU, Y. An infiltration method to synthesize thermoplastic polyurethane composites based on size-controlled graphene foams. ***Composites Part A: Applied Science and Manufacturing,*** v. 97, p. 67-75, 2017.

LEE, S.; EOM, T.; KIM, M.-K.; YANG, S.-G.; SHIM, B. S. Durable soft neural micro-electrode coating by electrochemical synthesis of PEDOT:PSS / graphene oxide composites. ***Electrochimica Acta,*** 2019.

LIU, L.; ZHANG, J.; ZHAO, J.; LIU, F. Mechanical properties of graphene oxides. ***Nanoscale,*** v. 4, n. 19, p. 5910, 2012.

LORENZETTI, Solange G.; QUEIROZ, A. A. A.; CAMILLO, Maria Aparecida Pires; HIGA, Olga Zazuco. Citotoxicidade do copolímero PEBD-e-PHEMA obtido por radiação ionizante. *In*: INTERNATIONAL NUCLEAR ATLANTIC CONFERENCE - INAC, 2005, Santos, SP. ***Anais* [...]**. INAC 2005.

NAGI, C. S.; OGIN, S. L.; MOHAGHEGHIAN, I.; CREAN, C.; FOREMAN, A. D. Spray deposition of graphene nano-platelets for modifying interleaves in carbon fiber reinforced polymer laminates. ***Materials & Design,*** 108831, 2020.

OLESIK, P.; GODZIERZ, M.; KOZIOL, M. Caracterização preliminar de novo composto resistente ao desgaste baseado em LDPE adequado para impressão 3D FDM. ***Materiais,*** v. 12 n. 16, 2520, 2019. DOI: 10.3390 / ma12162520

OWENS, N. F.; GINGELL, D.; TROMMLER, A. Cell adhesion to hydroxyl groups of a monolayer film. ***J Cell Sci.*** v. 91, Pt 2, p. 269-279, 1988.

PANDEY, A. K.; SINGH, K.; KAR, K. K. Thermo-mechanical properties of graphitereinforced high density polyethylene composites and its structure property corelationship. ***Journal of Composite Materials,*** v. 51, n. 12, p. 1769-1782, Dec. 2016.

PHILIPPE, B. Custom-made prefabricated titanium miniplates in le Fort i osteotomies: principles, procedure and clinical insights. ***International Journal of Oral and Maxillofacial Surgery,*** v. 42, n. 8, p. 1001-1006, 2013.

QASSEMYAR, Q.; ASSOULY, N.; TEMAN, S.; KOLB, F. Use of a three dimensional custom-made porous titanium prosthesis for mandibular body reconstruction. ***International Journal of Oral and Maxillofacial Surgery,*** v. 46, n. 10, p. 1248-1251, 2017.

QUILES-DÍAZ, S.; ENRIQUE-JIMENEZ, P.; PAPAGEORGIOU, D. G.; ANIA, F.; FLORES,A.; KINLOCH, I. A.; SALAVAGIONE, H. J. Influence of the chemical functionalization of graphene on the properties of polypropylene--based nanocomposites. ***Composites Part A: Applied Science and Manufacturing,*** 100, 31-39, 2017.

RAFIEE, M. A.; RAFIEE, J.; WANG, Z.; SONG, H.; YU, Z.-Z.; KORATKAR, N. Enhanced mechanical properties of nanocomposites at low graphene content. ***ACS Nano,*** v. 3, n. 12, p. 3884-3890, 2009.

REDIGHIERI, K. I. ***Estudos de compósitos de partículas de madeira e PEBD reciclado na presença de agentes compatibilizantes.*** Dissertação (Mestrado em Engenharia Química) - Universidade Federal Rural do Rio de Janeiro, 2006.

SLEZIONA, J. ***Podstawy technologii kompozytów.*** Gliwice, Poland: Wydawnictwo Politechniki Slaskiej. 1998.

TEGON, C. C. ***Pesquisa e desenvolvimento de nanocompósito constituído por poli (l-ácido láctico) e óxido de grafeno para impressão 3d de implantes de grau médico.*** Tese (Doutorado em Engenharia de Materiais) - Universidade Presbiteriana Mackenzie, São Paulo, 2021.

TIBBETTS, G.; LAKE, M.; STRONG, K.; RICE, B. A review of the fabrication and properties of vapor-grown carbon nanofiber/polymer composites. ***Composites Science and Technology,*** v. 67, n. 7-8, p. 1709-1718, 2007.

TRIVEDI, D. N.; RACHCHH, N. V. Graphene and its application in thermoplastic polymers as nano-filler. ***A Review.*** v. 240, 1 Feb. p. 124486, 2022.

YUAN, M.; XIONG, C.; JIANG, L.; LI, H.; YUAN, M. The preparation, characterization, mechanical and antibacterial properties of GO-ZnO nanocomposites with a poly(L-lactide)- modified surface. ***Materials,*** v. 11, n. 2, 2018.

YUSOF, M. A.; NOR RAHMAN, N. H.; IZIRWAN, I.; MAT DESA, M. S. Z.; AB GHANI, N. F. Development of graphene oxide/ Polyethylene to enhance mechanical properties through melt mixing technique. IOP Conference Series. ***Earth and Environmental Science,*** v. 1205, INTERNATIONAL SYMPOSIUM ON CIVIL AND ENVIRONMENTAL ENGINEERING, 4, 2023.

ZHOU, J.; WANG, Z.; ZHANG, S.; LIN, H.; GAO, C.; ZHAO, J., … WANG, X. Methionine and its hydroxyl analogs improve stem cell activity to eliminate deoxynivalenol-induced intestinal injury by reactivating wnt/β-catenin signaling. ***Journal of Agricultural and Food Chemistry,*** v. 67, n. 41, p. 11464-11473, 2019.

---

Received: 11 July 2023 - Accepted: 10 November 2023.